Turbulence, mixing and Prandtl number effects in stratified plane Couette flows

Qi Zhou[1], John Taylor[1] and Colm Caulfield[2,1]

[1]Department of Applied Mathematics and Theoretical Physics
[2]BP Institute,
University of Cambridge

Abstract

We report direct numerical simulations (DNS) of stratified plane Couette (SPC) flows in both continuous and layered stratifications for a wide range of Prandtl number Pr from 0.7, 7 to 70. In the continuously stratified set-up, Pr has a significant impact on the momentum and heat fluxes across the flow. Variations of these fluxes then modifies the turbulence characteristics in the way that is consistent with Monin–Okukhov (M-O) similarity theory. The mixing properties in the interior of the flow, however, appear to be independent of Pr. We employ M-O theory and the Osborn (1980) model to formulate scalings for the turbulent diffusivities. These scalings are then verified by DNS and discussed with respect to existing scalings in the literature. In the layered configuration, we investigate the transient mixing of a density interface, where the variation of Pr indeed becomes important.

1 Introduction

In this paper, we present a computational study of stratified plane Couette (SPC) flows. An SPC flow is bounded by two horizontal walls located at $y = \pm h$ respectively, and the walls move in opposite directions with a constant speed U_w. The temperature θ at the upper and lower walls is held at $\pm T_w$ respectively, and the fluid density ρ relates to θ via a linear equation of state $\rho = \rho_0(1 - \alpha_V\theta)$, which results in a stably stratified system. The three external parameters are Reynolds number $Re \equiv U_w h/\nu$, Richardson number $Ri \equiv \alpha_V T_w g h/U_w^2$ and Prandtl number $Pr \equiv \nu/\kappa$, where α_V is thermal expansion coefficient, g is gravity, ν is viscosity and κ is diffusivity. The direct numerical simulations (DNS) reported here are all for $Re = 4250$ and for varying Ri and Pr values. The DNS algorithm can be found in Taylor (2008), and the configurations of the SPC simulations are reported in Deusebio et al. (2015) and Zhou et al. (2016) (the latter is hereinafter referred to as 'ZTC').

Two configurations of SPC flows are examined in this paper, one being the fully developed statistically stationary turbulent SPC (§2), the other being a 'layered' set-up featuring a density interface introduced as an initial condition (§3). One common thread through these two configurations is the role of Prandtl number Pr. While most existing SPC studies have focused on Pr values of order unity (e.g., García-Villalba et al. (2011); Deusebio et al. (2015)), there has been growing evidence indicating that Pr can indeed have some first-order effects on stratified shear flows. For example, the effects of Pr on the characteristics of secondary instabilities and diapycnal mixing were reported by Salehipour et al. (2015) through simulations of growing Kelvin-Helmholtz instabilities. Motivated by these observations, we aim to investigate the effects of Pr systematically in SPC flows by varying Pr from 0.7, 7 to 70 (note the first two values correspond to the scenarios of heat in air and heat in water, respectively, and the third value is investigated

in an attempt to approach the large Schmidt number of salt in water, i.e., 700). The other common thread is to examine the diapycnal mixing characteristics of SPC flows: For the fully developed set-up, we propose a parameterization for the turbulent diffusivities based on Monin–Obukhov similarity theory and the Osborn (1980) formulation . Also presented are some preliminary results in the layered set-up where the transient mixing of a density interface is investigated.

2 Fully developed SPC flow

2.1 Effects of Prandtl number

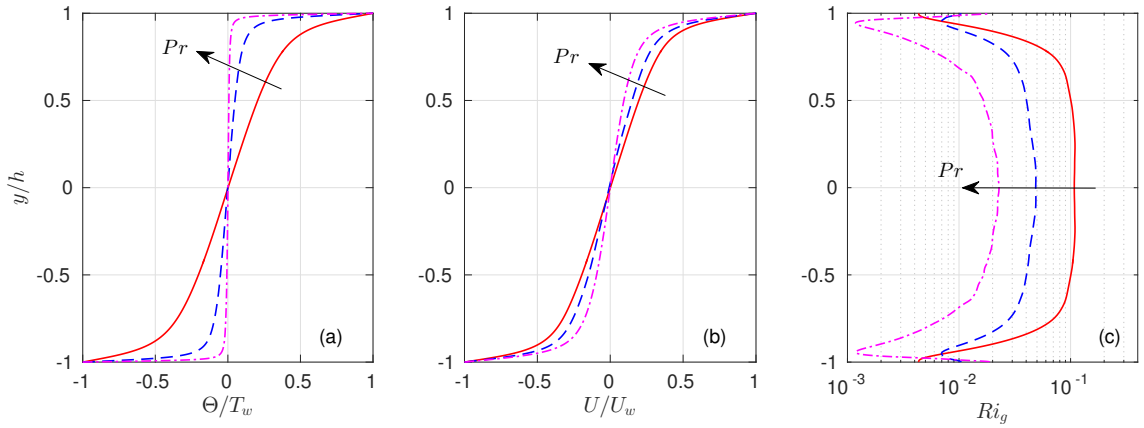

Figure 1: Vertical profiles of mean temperature Θ/T_w, mean velocity U/U_w and gradient Richardson number Ri_g at $(Re, Ri) = (4250, 0.04)$. For $Pr = 0.7$ plotted with a solid line; for $Pr = 7$ plotted with a dashed line; and for $Pr = 70$ plotted with a dot-dashed line. The oppositely moving walls are located at $y/h = \pm 1$ where h is the half channel height. Dirichlet boundary conditions for temperature $\theta = \pm T_w$ are applied at $y/h = \pm 1$ respectively. As Pr increases, sharpening of the near-wall temperature gradient $d\Theta/dy$ can be observed.

We first focus on the turbulent characteristics in the fully developed SPC flow. Figure 1 shows the effects of Pr on the mean velocity U and mean temperature Θ profiles in the wall-normal direction y. At fixed values of $(Re, Ri) = (4250, 0.04)$, the mean temperature gradient $d\Theta/dy$ (plotted in figure 1(a)) sharpens significantly in the near-wall region, as Pr increases by two orders of magnitudes from 0.7 to 70. On the other hand, the vertical variation of Θ weakens in the interior of the gap away from the walls with increasing values of Pr. The gradient Richardson number (plotted in figure 1(c)), is defined as

$$Ri_g(y) \equiv \frac{N^2}{S^2} = \frac{-(g/\rho_0)(d\overline{\rho}/dy)}{(dU/dy)^2} = \frac{g\alpha_V(d\Theta/dy)}{(dU/dy)^2}, \tag{1}$$

where $S \equiv dU/dy$ denotes the mean vertical shear and U is the mean velocity over the horizontal plane. Ri_g varies sharply in the near-wall region and reaches a plateau in the gap interior. Given that the mean shear S (plotted in figure 1(b)) is less sensitive to Pr, the Ri_g values at mid-gap ($y = 0$) decrease with Pr at fixed values of (Re, Ri), which is attributed to the sharpening of $d\Theta/dy$ in the near-wall region and weakening of those gradients (and thus the strength of stratification, as measured by N^2) in the gap interior. This suggests that varying Pr reshapes the mean temperature and velocity profiles which results in smaller Ri_g values in the gap interior, allowing shear to dominate stratification away from the walls. As is discussed in detail by ZTC, increasing Pr also moves the

intermittency boundary in SPC flows (Deusebio et al., 2015), i.e., the largest Ri that supports fully developed turbulence for a given Re, towards larger values of Ri, which is due to the modifications of momentum and heat fluxes at the wall due to varying Pr.

2.2 Monin–Obukhov similarity scaling

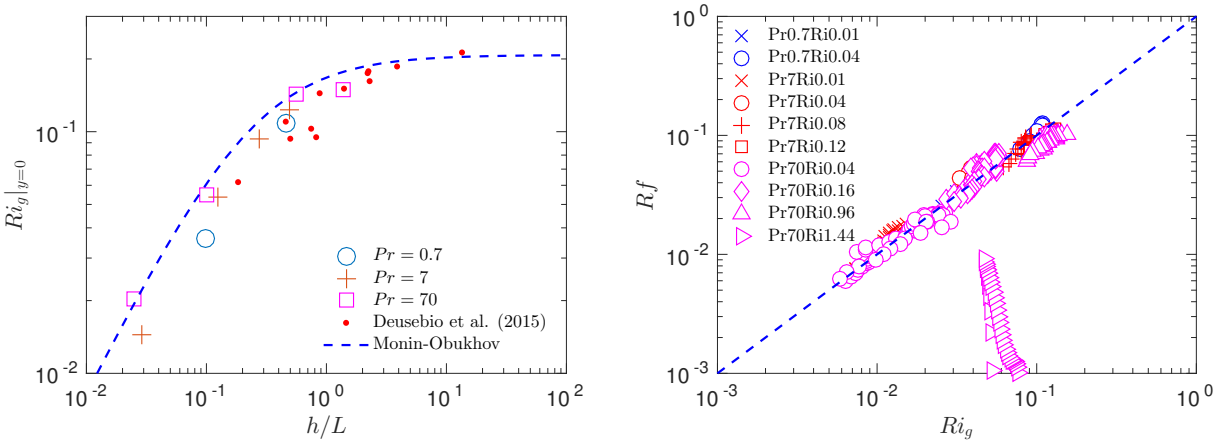

Figure 2: Left panel: Equilibrium gradient Richardson number $Ri_g|_{y=0}$ at mid-gap, as a function of length scale ratio h/L. Right panel: Flux Richardson number $Rf \equiv -B/P$ as a function of gradient Richardson number Ri_g. Rf and Ri_g values are computed pointwise in y in the gap interior with $y^+ \equiv y_w u_\tau/\nu > 50$, where y_w is the wall-normal distance. For the group of outliers on the right panel, i.e., $(Pr, Ri) = (70, 1.44)$, the flow is viscously controlled with Re_b values of approximately 20.

Such effects of varying Pr on the mean flow can be rationalized by a mixing length model (see details in ZTC) which incorporates Monin–Obukhov (M-O) similarity theory and near-wall corrections (van Driest, 1956). As discussed by ZTC, M-O theory also provides a framework to formulate some key scalings for the SPC turbulence. Two of those similarity scalings are shown in figure 2. It can be shown via M-O theory that the Ri_g value at mid-gap ($y = 0$) can be written as

$$Ri_g|_{y=0} = \frac{k_m}{k_s} \frac{(h/L)^{-1} + \beta_s}{[(h/L)^{-1} + \beta_m]^2}, \tag{2}$$

where k_m, k_s, β_m and β_s are all dimensionless constants in M-O theory, and L is the Obukhov length scale which is defined as

$$L \equiv \frac{u_\tau^3}{k_m g \alpha_V q_w}, \tag{3}$$

where u_τ is the friction velocity, k_m is the von Karman constant for momentum, and q_w is the heat flux through the wall. Note (2) has no explicit dependence on Pr, and the scaling seems to be in agreement with DNS data at a wide range of Pr values, as shown in the left panel of figure 2. The indirect effects of Pr on the interior turbulence is through the modulation of the wall momentum flux u_τ^2 and heat flux q_w which are present in (3), the expression for L. As shown in figure 2, when h/L is $O(1)$ or smaller, the equilibrium Ri_g at mid-gap varies strongly with h/L. Under this scenario, the stabilising effects due to stratification are relatively weak. When $h/L \to \infty$, the mid-gap equilibrium Ri_g saturates at

$$Ri_g|_{y=0} = \frac{k_m}{k_s} \frac{\beta_s}{\beta_m^2} \simeq 0.21, \tag{4}$$

a scenario analogous to the discussion of constant-flux layers in 'very stable' stratification (Ellison, 1957; Turner, 1973).

As shown in the right panel of figure 2, the other important feature that is due to the M-O similarity is that the flux Richardson number $Rf \equiv -B/P$ scales linearly with the gradient Richardson number Ri_g for fully developed turbulent SPC flows. Here B is buoyancy flux and P is shear production. In other words, the turbulent Prandtl number $Pr_t \equiv \nu_t/\kappa_t = Ri_g/Rf$ is order unity, where $\nu_t \equiv -\langle u'v'\rangle/S$ are $\kappa_t \equiv -\langle \rho'v'\rangle/(d\overline{\rho}/dy)$ the turbulent diffusivities of momentum and density respectively.

2.3 Parameterization of turbulent diffusivities

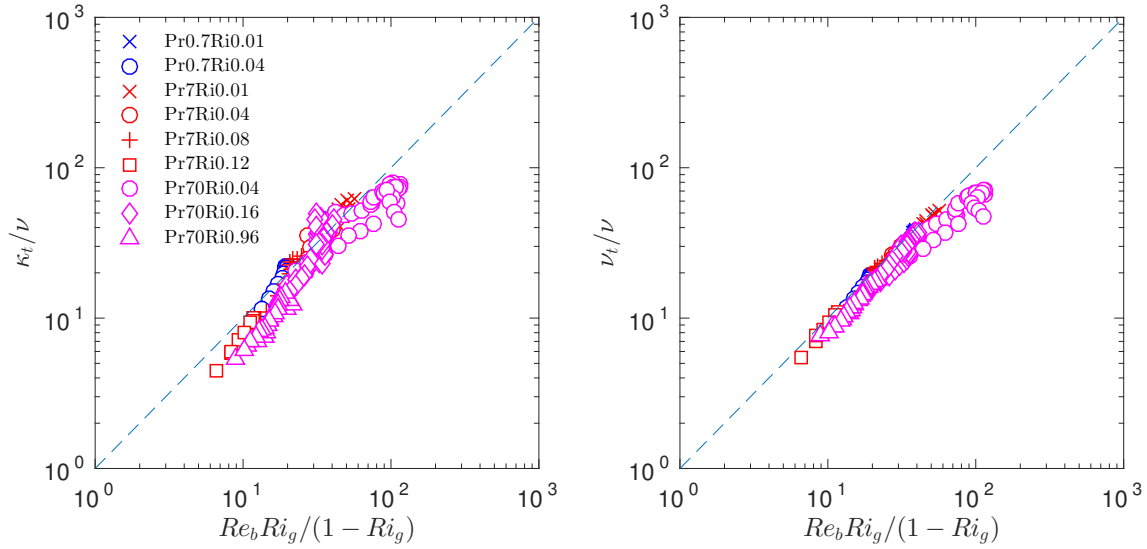

Figure 3: κ_t and ν_t, both normalised by ν, as a function of $Re_b Ri_g/(1-Ri_g)$. κ_t, ν_t, Re_b and Ri_g values are computed pointwise in y in the gap interior with $y^+ > 50$.

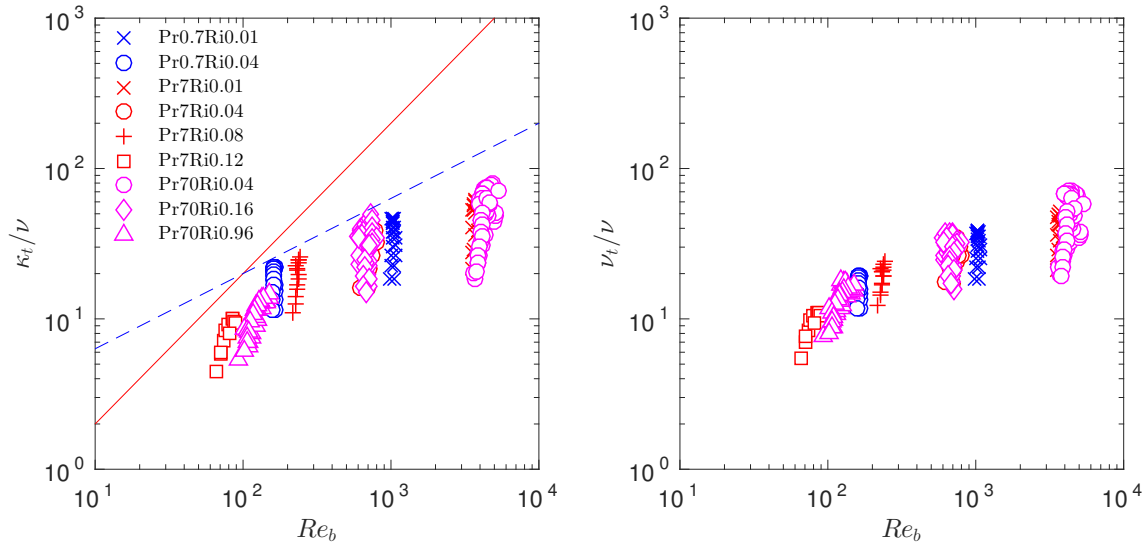

Figure 4: κ_t and ν_t, both normalised by ν, as a function of Re_b. Scaling laws of $\kappa_t/\nu = 0.2Re_b$ (Osborn, 1980) plotted with a solid line, and $\kappa_t/\nu = 2Re_b^{1/2}$ (Shih et al., 2005) plotted with a dashed line, are also shown.

We proceed by formulating a parameterization of the turbulent diffusivity κ_t in SPC flows away from the walls. Following Osborn (1980), the steady-state turbulent kinetic energy

balance $P \approx \varepsilon - B$ (where ε is dissipation) leads to

$$\frac{\kappa_t}{\nu} \approx \frac{Rf}{1-Rf}\frac{\varepsilon}{\nu N^2} = \Gamma Re_b, \tag{5}$$

where $Re_b \equiv \varepsilon/(\nu N^2)$ is the buoyancy Reynolds number, and $\Gamma \equiv B/\varepsilon \approx Rf/(1-Rf)$ is the turbulent flux coefficient. It is a fundamental question how Γ (commonly referred to as 'mixing efficiency' in the oceanographic literature) is to be parameterized (see e.g. Ivey et al. (2008)). As is shown in figure 2, $Rf \simeq Ri_g \lesssim 0.2$ in SPC flows for turbulence to be maintained. Indeed, using this scaling, Γ can be written as a function of the gradient Richardson number Ri_g:

$$\Gamma \approx \frac{Ri_g}{1-Ri_g}. \tag{6}$$

As Pr_t is order unity, one expects ν_t to follow the same scalings as κ_t. Figure 3 compares these scalings against DNS data and shows reasonable agreement for all Prandtl numbers investigated. The collapse of data, when the Ri_g-dependence in Γ is included as in (6), has improved from the parameterizations that involves only the buoyancy Reynolds number Re_b (plotted in figure 4) in the power-law form, i.e., $\kappa_t/\nu \sim Re_b^n$.

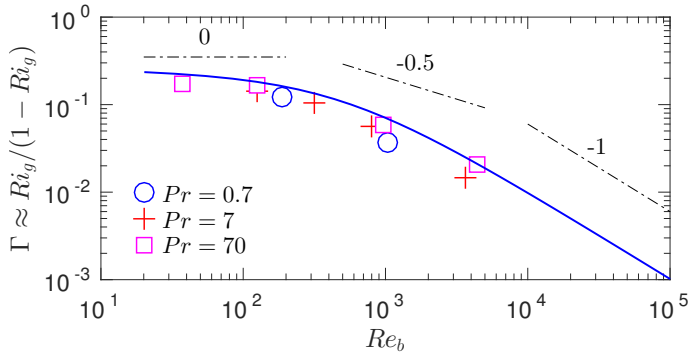

Figure 5: Turbulent flux coefficient Γ approximated by $Ri_g/(1-Ri_g)$, where Ri_g is evaluated at mid-gap, plotted as a function of Re_b which is approximated by $k_m L^+$ (where $L^+ \equiv Lu_\tau/\nu$; see ZTC for more details on the approximation). Symbols correspond to DNS data. Solid line corresponds to Monin-Obukhov predictions at $Re = 4250$. Power-law scalings $\Gamma \propto Re_b^n$ are plotted with dot-dashed lines marked with the various values of n.

The scaling for Γ shown in (6), which is based on M-O theory, also provides a convenient framework to interpret the reported change of power-law exponent in Re_b in the scaling of Γ, e.g., as reported by Barry et al. (2001); Shih et al. (2005). This is demonstrated in figure 5, where the characteristic values of turbulent flux coefficient Γ in the interior of SPC flow are plotted against the corresponding Re_b values. The M-O predictions from the mixing length model presented in ZTC are also shown.

As shown in figure 5, when Re_b is smaller than $O(100)$, which corresponds to the $h/L > 1$ regime in terms of the characteristic Ri_g value (see figure 2(a)), Ri_g remains a constant value of approximately 0.2 at mid-gap as given in (4). The characteristic turbulent flux coefficient $\Gamma \approx 0.25$ is thus a constant. This regime is reminiscent of Shih et al. (2005)'s 'intermediate' regime where Γ is a constant of 0.2 independent of Re_b. Consequently, $\kappa_t/\nu = \Gamma Re_b \propto Re_b$ in this regime. This regime may be thought of as a saturated regime for Γ, as Ri_g is close to its maximum value for sustained turbulence. This is consistent with the underlying assumptions of Osborn (1980) who argued that $\Gamma \lesssim 0.2$ based on the

theory of Ellison (1957) and the experiment of Britter (1974), both of which concerning wall-bounded flows.

When Re_b is large, e.g. $Re_b > O(1000)$ for $Re = 4250$, which corresponds to the $h/L \ll 1$ limit in terms of Ri_g (figure 2(a)), it can be shown (see in ZTC) that the characteristic Ri_g scales as $Ri_g \approx (k_m^2/k_s)(Re_{\tau,\infty}/Re_b)$, where $Re_{\tau,\infty}$ is the friction Reynolds number for the case of passive scalar ($Re_b \to \infty$). With $Ri_g \ll 1$ in this limit, $\Gamma \approx Ri_g/(1 - Ri_g) \approx Ri_g$. It follows that $\Gamma \approx Ri_g \propto Re_b^{-1}$ holds for large Re_b in the limit of zero stratification, and, in this limit of $Re_b \to \infty$, $\kappa_t/\nu = \Gamma Re_b = k_m^2 k_s^{-1} Re_{\tau,\infty}$ approaches a constant which depends solely on $Re_{\tau,\infty}$ (which itself is a function of the bulk Reynolds number Re). This regime finds no counterpart in the regimes presented in Shih et al. (2005). As is apparent in figure 5, this regime only really becomes clearly identifiable for $Re_b \gtrsim 1000$, larger values than those presented in Shih et al. (2005).

There exists a transitional regime where Γ decays monotonically with Re_b, but with a slower rate than the $\Gamma \propto Re_b^{-1}$ power law in the weakly stratified limit. This transitional regime at least superficially resembles Shih et al. (2005)'s 'energetic' regime where $\Gamma \propto Re_b^{-1/2}$ and $\kappa_t/\nu \propto Re_b^{1/2}$. The critical Re_b which marks the transition from the small-Re_b regime to this intermediate-Re_b regime, appears to be approximately 100 for $Re = 4250$.

3 Layered SPC flow

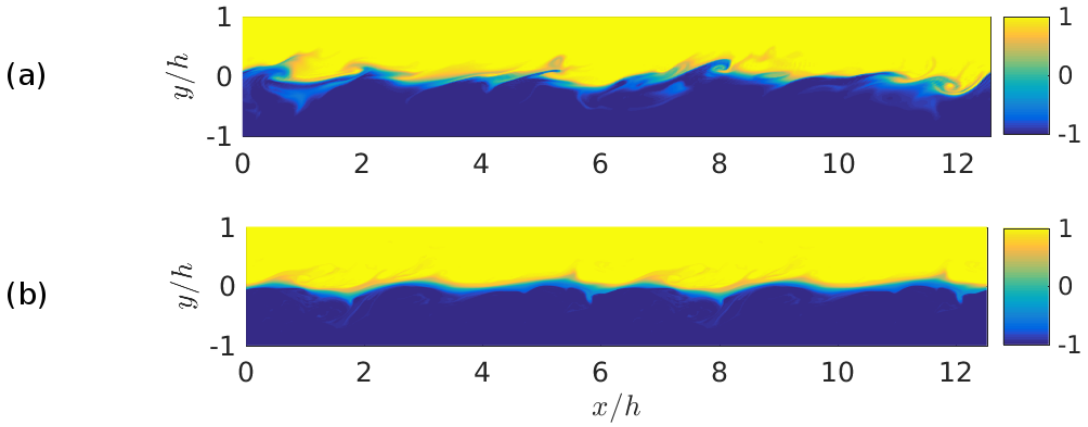

Figure 6: Snapshots of the active scalar (temperature θ, which is normalized by T_w) field in layered SPC flows at $Re = 4250$ on a along-stream/vertical (xy) transect. Panel (a) shows the case $(Pr, Ri) = (7, 0.04)$ at $t = 8.7$, and panel (b) shows the case $(Pr, Ri) = (70, 0.32)$ at $t = 96$ (the field is repeated in the periodic direction x for visualization). The oppositely moving walls are located at $y/h = \pm 1$, and the density interface is introduced at $t = 0$. t is normalized by the advective time unit h/U_w.

The second configuration considered here is the mixing of a density interface in SPC flow. By introducing the interface as an initial condition, we are able to examine a wider range in terms of Richardson number, i.e., $Ri_g > 0.2$, where the density flux is often expected to vary non-monotonically with stratification (Phillips, 1972; Linden, 1979). Some qualitative features of the density interface are shown in figure 6. When Ri is small, the interface overturns due to the imposed shear which induces vigorous mixing, e.g., as shown in figure 6(a). When Ri and Pr are both sufficiently large, however, structures strongly reminiscent of 'Holmboe waves' appear to develop on the interface, and these structures prove to be long-lived and robust (see figure 6(b)). Interestingly, the interface remains sharp in this particular 'Holmboe' regime, despite the turbulence

external to the interface, as well as molecular diffusion. Ongoing research efforts are devoted to understanding the physical mechanism that 'sharpens' the interface which seems to be exclusive to the large-Pr simulations.

4 Conclusions

In this paper, we have presented the numerical data from two configurations of stratified plane Couette (SPC) flows, i.e., the fully developed (§2) and layered (§3) set-ups, aiming at the effects of Prandtl number Pr and characteristics of diapycnal mixing. In the fully developed case, the effect of varying Pr is in modulating the wall fluxes of momentum and buoyancy which are key quantities in the self-similar scaling of the turbulence. Employing Monin–Obukhov theory, we have established an upper bound for the gradient Richardson number Ri_g in the gap interior, i.e., $Ri_g \lesssim 0.2$. For the range of Ri_g that is accessible in the fully developed turbulence, we have found that the flux Richardson number Rf scales linearly with Ri_g, which results in the Ri_g-based scaling for the turbulent flux coefficient Γ, following the classical formulation of Osborn (1980). We have extended the investigation to larger Richardson numbers in the layered set-up in an attempt to examine the nonmonotonic mixing behaviour (Phillips, 1972; Linden, 1979). The possibility of having a self-sustained 'Holmboe' regime where a density interface remains sharp subject to the effect of external turbulence, has been confirmed. Preliminary results are highly suggestive that large Prandtl number plays a key role in modifying the mixing characteristics of these interfaces.

Acknowledgement

This work is supported by UK EPSRC Programme Grant EP/K034529/1 entitled 'Mathematical Underpinnings of Stratified Turbulence' (MUST).

References

Barry, M. E., Ivey, G. N., Winters, K. B., and Imberger, J. (2001). Measurements of diapycnal diffusivities in stratified fluids. *J. Fluid Mech.*, 442:267–291.

Britter, R. (1974). *An experiment on turbulence in a density stratified fluid*. PhD thesis, Monash University, Victoria, Australia.

Deusebio, E., Caulfield, C. P., and Taylor, J. R. (2015). The intermittency boundary in stratified plane Couette flow. *J. Fluid Mech.*, 781:298–329.

Ellison, T. (1957). Turbulent transport of heat and momentum from an infinite rough plane. *J. Fluid Mech.*, 2:456–466.

García-Villalba, M., Azagra, E., and Uhlmann, M. (2011). Mixing efficiency in stably-stratified plane Couette flow. In *Proceedings of the 7th Int. Symp. on Stratified Flows, Rome, Italy*.

Ivey, G. N., Winters, K. B., and Koseff, J. R. (2008). Density stratification, turbulence, but how much mixing? *Annu. Rev. Fluid Mech.*, 40:169.

Linden, P. F. (1979). Mixing in stratified fluids. *Geophys. Astro. Fluid Dyn.*, 13:3–23.

Osborn, T. R. (1980). Estimates of the local rate of vertical diffusion from dissipation measurements. *J. Phys. Oceanogr.*, 10:83–89.

Phillips, O. M. (1972). Turbulence in a strongly stratified fluid – is it unstable? *Deep-Sea Res.*, 19:79–81.

Salehipour, H., Peltier, W., and Mashayek, A. (2015). Turbulent diapycnal mixing in stratified shear flows: the influence of Prandtl number on mixing efficiency and transition at high Reynolds number. *J. Fluid Mech.*, 773:178–223.

Shih, L. H., Koseff, J. R., Ivey, G. N., and Ferziger, J. H. (2005). Parameterization of turbulent fluxes and scales using homogeneous sheared stably stratified turbulence simulations. *J. Fluid Mech.*, 525:193–214.

Taylor, J. R. (2008). *Numerical Simulations of the Stratified Oceanic Bottom Boundary Layer*. PhD thesis, University of California, San Diego.

Turner, J. S. (1973). *Buoyancy Effects in Fluids*. Cambridge University Press.

van Driest, E. R. (1956). On turbulent flow near a wall. *J. Aeronaut. Sci.*, 23:1007–1011.

Zhou, Q., Taylor, J. R., and Caufield, C. P. (2016). Self-similar mixing in stratified plane couette flow for varying prandtl number. Submitted to *J. Fluid Mech.*, referred to in the text as 'ZTC'.